Heat Shock Protein 27 as a New Therapeutic Target for Radiation Sensitization of Head and Neck Squamous Cell Carcinoma

Elie Hadchity[1,2], Marie-Thérèse Aloy[1,2], Christian Paulin[1–4], Emma Armandy[1,2], Emmanuel Watkin[1,5], Robert Rousson[1,3,6], Martin Gleave[7], Olivier Chapet[1,3,8] and Claire Rodriguez-Lafrasse[1–3,9]

[1]Université de Lyon, Université Lyon-I, Lyon, France; [2]Laboratoire de Radiobiologie Cellulaire et Moléculaire, EA-3738, Faculté de Médecine Lyon-Sud, Oullins, France; [3]Hospices Civils de Lyon, Lyon, France; [4]Laboratoire d'Anatomie et de Cytologie Pathologiques, Pierre Bénite, France; [5]Ciblage Thérapeutique en Oncologie, EA-3738, Oullins, France; [6]Laboratoire de Biochimie, Centre de Biologie Est, Lyon, France; [7]The Prostate Centre, Vancouver General Hospital, Department of Urological Sciences, Vancouver, British Columbia, Canada; [8]Service de Radiothérapie, Pierre Bénite, France; [9]Laboratoire de Biologie des Tumeurs, Pierre Bénite, France

In a wide range of human cancers, increased levels of heat shock protein 27 (Hsp27) are closely associated with tumorigenesis, metastasis, resistance to anticancer therapeutics, and thus poor prognosis. In this study, we evaluate the radiosensitizing effects of Hsp27 gene silencing using OGX-427, a second-generation antisense oligonucleotide (ASO), on the radioresistant head and neck squamous cell carcinoma (HNSCC) SQ20B cells. *In vitro*, the downregulation of Hsp27 significantly enhanced radiation-induced apoptotic and clonogenic death, and promoted Akt inactivation. *In vivo*, combining OGX-427 with local tumor irradiation (5 × 2 Gy) led to a significant regression of SQ20B tumors related to a high rate of apoptosis and decreased levels of glutathione antioxidant defenses. Increasing the total radiation dose (15 × 2 Gy) significantly amplified the radiosensitizing effect of OGX-427. Treatment of tumors with OGX-427 plus radiation resulted in a decrease in angiogenesis associated with a reduced activation of the Akt pathway. Furthermore, the combined treatment enhanced the survival of SQ20B-bearing mice and showed no signs of acute and delayed toxicity. Our findings demonstrate for the first time that Hsp27 knockdown enhances the cytotoxic effects of radiotherapy *in vivo* and provide preclinical proof of principle for clinical trials using Hsp27 antisense technology in the treatment of patients with HNSCC radioresistant cancers.

Received 28 November 2008; accepted 30 March 2009; published online 12 May 2009. doi:10.1038/mt.2009.90

INTRODUCTION

Head and neck squamous cell carcinoma (HNSCC) is the sixth most frequently occurring cancer in the world. Radiotherapy plays an important role in the management of affected patients and has for a long time been the primary treatment offered to those with inoperable disease. New therapeutic strategies have recently emerged including improved radiotherapy techniques (fractionated and intensity-modulated radiotherapies), alternating or concurrent chemoradiotherapy regimens, and the integration of targeted biological therapy.[1] Despite these significant improvements, the 5-year survival rate of 35% is one of the lowest associated with the main cancers, owing to the frequent relapse of the disease after primary therapy. New therapeutic concepts are therefore much needed to overcome the HNSCC resistance to anticancer treatments. One option involves the inhibition of physiological proteins with antiapoptotic properties, such as heat shock protein 27 (Hsp27). High levels of its expression have been detected in many human cancers including those of the prostate,[2] breast,[3] gastric,[4] and bladder.[5] Hsp27 was also recently identified as one of 41 proteins commonly overexpressed in tumors from HNSCC patients.[6] Moreover, Hsp27 overexpression has been widely associated with metastasis,[7] poor prognosis,[8] and short survival duration.[3] By its chaperone and antiapoptotic properties, Hsp27 contributes to the resistance of tumor cells to chemotherapy and radiotherapy.[9–11] In particular, Hsp27 can protect tumor cells against oxidative stress through a glucose-6-phosphate-dehydrogenase dependent ability to increase and maintain glutathione in its reduced form and also through its *in vivo* chaperone activity against oxidized proteins.[12] Thus, reducing antioxidant defenses of tumors by Hsp27 inhibition should increase cytotoxic efficiency of radiotherapy and improve clinical outcome. Furthermore, Hsp27 is involved in the regulation of the serine/threonine kinase Akt, an important signaling molecule for cell survival.

We previously reported the absence of significant apoptosis in response to irradiation[13] and the overexpression of Hsp27 protein in the basal state or after irradiation[14] in SQ20B cells, a radioresistant HNSCC cellular model. We further demonstrated the radiosensitizing effects of Hsp27 gene silencing in HNSCC, glioblastoma (U87), and prostate cancer cells (PC3), thus illustrating the clinical potential of Hsp27 inhibition as an adjuvant of radiotherapy.[14] In this study, we propose a preclinical proof of principle for the use of Hsp27 gene silencing by OGX-427 associated with radiotherapy in the treatment of radioresistant HNSCC.

Correspondence: *Claire Rodriguez-Lafrasse, Laboratoire de Radiobiologie Cellulaire et Moléculaire, EA-3738, Faculté de Médecine Lyon-Sud, BP12, 69921 Oullins Cedex, France. E-mail: claire.rodriguez@sante.univ-lyon1.fr*

RESULTS

Hsp27 knockdown by OGX-427 sensitizes SQ20B cells to γ-irradiation by increasing apoptotic and clonogenic cell death, and decreasing Akt activation

Before undertaking *in vivo* studies, we investigated the capacity of OGX-427 to improve the cytotoxicity of radiation in SQ20B cultured cells. SQ20B cells were incubated during 4 hours, for 2 consecutive days, with 200 nmol/l of either OGX-427 or mismatch oligonucleotide (MS) as a control, and then irradiated at different doses. As depicted in **Figure 1a**, western blot analysis revealed a transient overexpression of Hsp27 of 45 and 82%, respectively, at 30 minutes and 1 hour following 10 Gy irradiation in SQ20B-control and SQ20B-MS cells while it returned at a basal level until 48 hours postirradiation. A 90% decrease of Hsp27 expression was measured in SQ20B–OGX-427 cells compared to SQ20B-MS-control cells (**Figure 1b**). Thus, OGX-427 treatment inhibits both constitutive and radiation-induced expression of Hsp27.

Finally, no significant variation of Hsp70 and Hsp90 protein expression levels was observed in SQ20B-MS-control and OGX-427 transfected cells.

To test the radiosensitizing effect of OGX-427, cell survival curves were then established after irradiation of SQ20B–OGX-427 and SQ20B-MS-control cell lines at doses varying between 0.5 and 8 Gy. Transient transfection with OGX-427 increased the clonogenic cell death revealed in **Figure 1c** by an exponential decrease in the percentage of surviving cells. The survival fraction at 2 Gy, used as an index of radiosensitivity, shifted from 0.72 in SQ20B-MS-control cells to 0.48 in SQ20B–OGX-427 cells. Hsp27 inhibition was also associated with an increase of apoptotic cell death, as demonstrated by total caspase activation (**Figure 1d**) reaching up

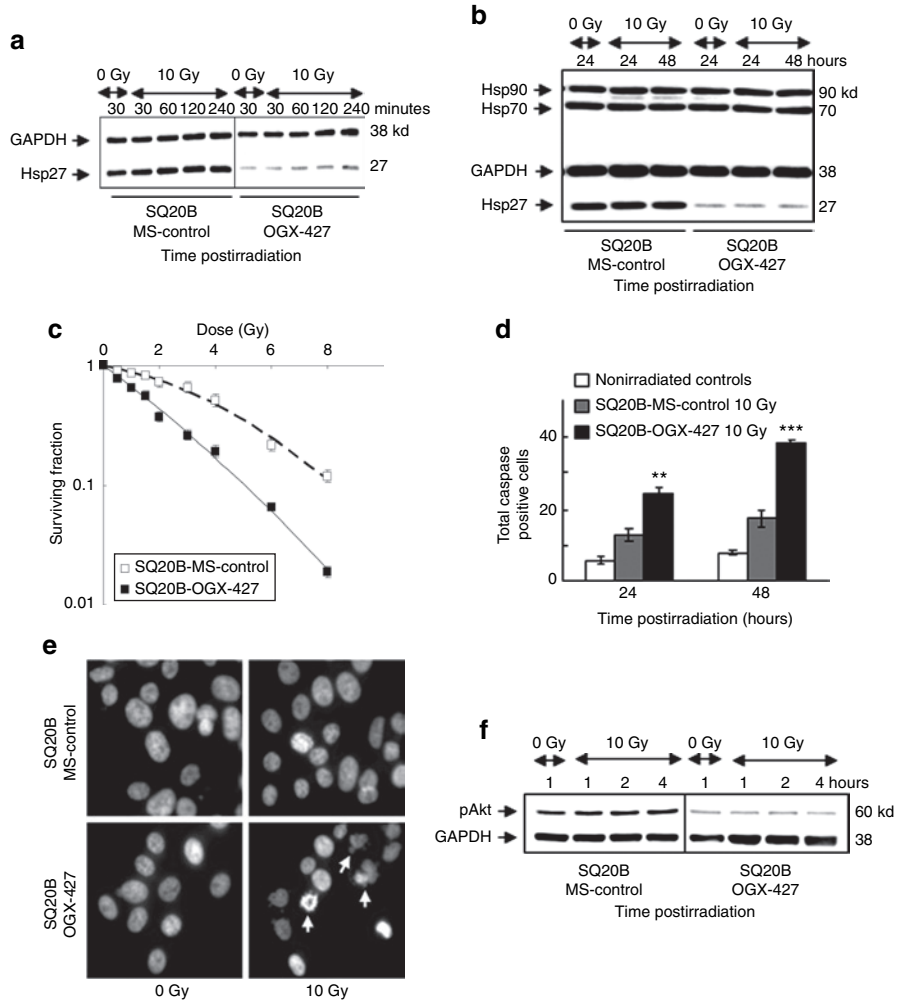

Figure 1 Knockdown of Hsp27 by OGX-427 sensitizes SQ20B cells to irradiation. (**a**) Immunoblot analysis of Hsp27 expression in response to 0 or 10 Gy irradiation of SQ20B-MS-control and SQ20B–OGX-427 cells. (**b**) Immunoblot analysis of Hsp27, Hsp70, and Hsp90 protein expression in response to 0 or 10 Gy irradiation. Protein (10 µg) was loaded on the gels. Glyceraldehyde-3-phosphate-deshydrogenase (GAPDH), as loading control. (**c**) Cell survival after exposure of SQ20B-MS-control and SQ20B–OGX-427 cell lines to radiation at doses varying between 0 and 8 Gy. Colonies with >64 cells were scored after six cell divisions following irradiation. (**d**) Total caspase activity quantified by flow cytometry. Each value represents the mean ± SD of two experiments performed in triplicate. $^{**}P < 0.005$, $^{***}P < 0.001$ versus irradiated SQ20B-MS-control cells. Nonirradiated controls represent the mean of results (triplicate) obtained in basal conditions for each transfected cell line. (**e**) Fluorescent DAPI staining examined 48 hours postirradiation. Apoptotic cells appear with characteristic disintegrated chromatin in the nuclei (white arrows) (original magnification ×40). (**f**) Immunoblot analysis of the phosphorylated active form of Akt (pAkt) in response to 0 or 10 Gy irradiation of SQ20B-MS-control and SQ20B–OGX-427 cells. DAPI, 4′-6-diamidino-2-phenylindole-dihydrochloride; GAPDH, glyceraldehyde-3-phosphate-dehydrogenase; Hsp, heat shock protein.

to 205% over MS-control irradiated cells ($P < 0.001$) at 48 hours postirradiation. These data were confirmed by the morphologic apoptotic changes shown by using 4′-6-diamidino-2-phenylindole-dihydrochloride staining at 48 hours postirradiation (**Figure 1e**).

Because Hsp27 can activate the pro-survival kinase Akt[15,16] through its phosphorylation on Ser[473] by the phosphatidylinositol-3-kinase,[17,18] we next investigated whether Hsp27 knockdown could lead to a reduced expression of the phosphorylated active form of Akt (pAkt). According to our hypothesis, we observed a decrease of pAkt in OGX-427 transfected cells whether irradiated or not (**Figure 1f**).

Thus, these preliminary *in vitro* results indicate that OGX-427 treatment sensitizes SQ20B cultured cells to irradiation by increasing apoptotic and clonogenic cell death, and by decreasing activation of the Akt survival pathway.

Hsp27 knockdown enhances radiation-induced regression of SQ20B xenograft tumors without significant toxicity, and increases mice survival

Figure 2a shows the tumor evolution in the six groups of mice from experiment I and illustrates the absence of a significant effect of MS treatment. Compared to the progressive and massive increase in tumor volume observed in the control groups [phosphate-buffered saline (PBS)-alone, MS-control], 10 Gy radiation stabilized tumor evolution between the second and the third week. The tumors then started to develop again with a growth curve resembling that of the control groups. In contrast, the combination of OGX-427 with 10 Gy radiation drastically enhanced the sensitivity of SQ20B tumors to the irradiation. At the end of treatment (week 6), the mean tumor volume had decreased by 485% compared to the control group and by 350% compared to irradiated control groups ($P < 0.001$). In our experimental conditions using high tumor volume (300–400 mm^3) as starting point for the treatment, OGX-427 alone had an almost insignificant effect on tumor growth.

To check whether the extension of radiotherapy treatment was associated with the improved effectiveness of the combined treatment, we conducted a second experiment (experiment II) in which the total radiation dose was increased to 30 Gy. In the absence of significant differences in tumor evolution observed during the first experiment between the control groups, the second experiment was conducted on three groups of mice only: PBS-alone, PBS + 30 Gy, and OGX-427 + 30 Gy.

Increasing the total dose of radiation in combination with OGX-427 resulted in an even greater inhibition of tumor growth (**Figure 2b**). At the end of week 6, the mean reduction in tumor volume was 720 and 500% ($P < 0.001$) compared, respectively, to the PBS-control and only irradiated tumors. These results are illustrated in **Figure 2c** by photos of one representative tumor taken from each group at week 6. Increasing the radiation dose delayed the restart of tumor growth, as shown by a tumor volume at the end of week 11 comparable to that at week 7 in the first study.

Western blot analysis at the end of treatment (week 6) revealed a significant downregulation of Hsp27 expression in OGX-427 treated tumors by up to 65% compared to the untreated control group (**Figure 2d**). No significant variation in the levels of Hsp70 and Hsp90 protein in tumors from all groups of the two experiments was observed.

An increase in the overall survival of mice, as represented by the Kaplan–Meyer curves for mice from experiment II, confirmed

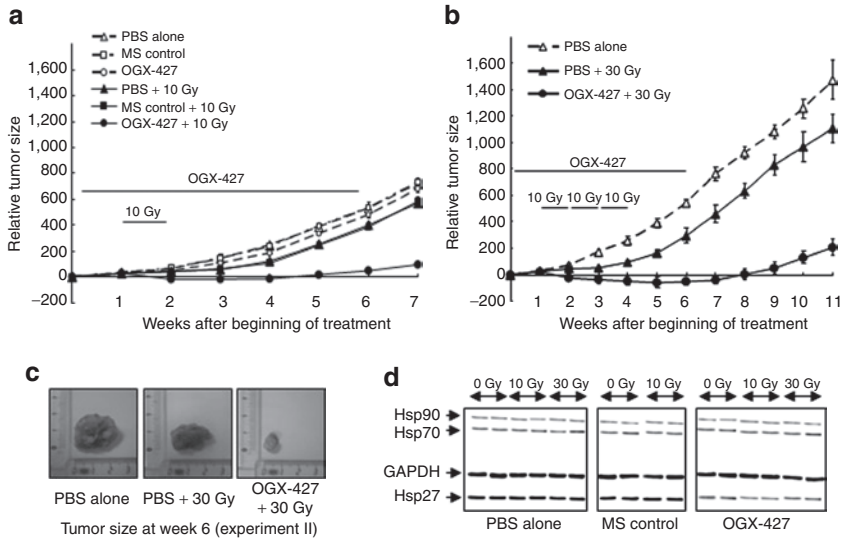

Figure 2 Combined treatment of OGX-427 with irradiation enhances the regression of SQ20B xenografted tumors. Mice bearing SQ20B tumors were randomly selected for treatment with PBS, 10 mg/kg of MS-control or OGX-427 injected once daily for 5 consecutive days (week 1) then three times per week for 5 weeks, associated or not with local tumor irradiation for a total dose of 10 or 30 Gy delivered at a daily dose of 2 Gy. (**a**) Tumor evolution after treatment with PBS, MS-control or OGX-427 oligonucleotides associated or not with 10 Gy radiation (week 2, experiment I). (**b**) Tumor evolution after treatment with PBS associated or not with 30 Gy irradiation, and OGX-427 plus 30 Gy (weeks 2, 3, and 4, experiment II). Tumor volume was measured once weekly and results were expressed as mean ± SD relative to that measured at the beginning of treatment. (**c**) Tumor specimen photos representative of each group of mice at the end of the treatment (experiment II). (**d**) Immunoblot analysis of Hsp27, Hsp70, and Hsp90 proteins in SQ20B xenografted tumors at the end of treatment for all experimental groups (two different tumors from each group). Protein (2 µg) was loaded on the gels. GAPDH, glyceraldehyde-3-phosphate-dehydrogenase; Hsp, heat shock protein; PBS, phosphate-buffered saline.

the efficacy of the treatment. The viability was followed up to week 24 following the beginning of treatment. None of the mice from the untreated group survived after the 14th week whereas 30 Gy treatment prolonged the lifespan to the 18th week and the combined treatment to past the 24th week (**Figure 3a**).

To determine the systemic toxicity of the various treatments, body weight was recorded among all experimental groups of the two studies. As shown in **Figure 3b,c**, only the untreated groups showed a mild loss in body weight (<15% of the pretreatment value). The irradiation alone or combined with OGX-427 was well tolerated and showed no sign of acute and delayed toxicity. The tissue morphology of liver, lung, brain, and skeletal muscle surrounding the tumor, performed with hematoxylin–phloxine–saffron staining, was similar between the different groups of treated mice (**Figure 3d**).

The overall results demonstrate that Hsp27 knockdown by OGX-427 treatment markedly improves the response of HNSCC tumors to radiotherapy without significant toxicity.

Combined treatment by OGX-427 and radiation increases apoptotic cell death and decreases glutathione levels and angiogenesis

Terminal nucleotidyl transferase–mediated nick end labeling staining (**Figure 4a**) of tumor sections confirmed the results obtained *in vitro*. No significant induction of apoptosis was displayed in SQ20B xenografts treated with either OGX-427 alone (**Figure 4a**) or the MS-control (data not shown). Radiation alone led to only a slight increase in the number of apoptotic cells whereas the combined treatment of OGX-427 and radiation resulted in large fields of apoptosis. Increasing the total dose of radiation from 10 to 30 Gy without changing the OGX-427 treatment led to an even greater increase in the apoptotic rate. These results were confirmed in experiment II by immunostaining of the cleaved-caspase-3. The proportion of active-caspase-3 expressing cells was higher in tumors treated with the combination of OGX-427 and irradiation compared to those only irradiated.

Because Hsp27 protects tumor cells against oxidative stress by increasing levels of glutathione and maintaining it in its reduced form, we further verified that the tumor glutathione levels were affected by the combined treatment with OGX-427 and radiation. The combined treatment led to a significant decrease in intratumoral total glutathione levels, most pronounced at the highest dose of radiation, of 68 and 59%, respectively, compared to the untreated and 30 Gy irradiated alone mice groups ($^*P < 0.05$) (**Figure 4b**).

Finally, we investigated any association between tumor growth inhibition and an alteration of tumor proliferation and

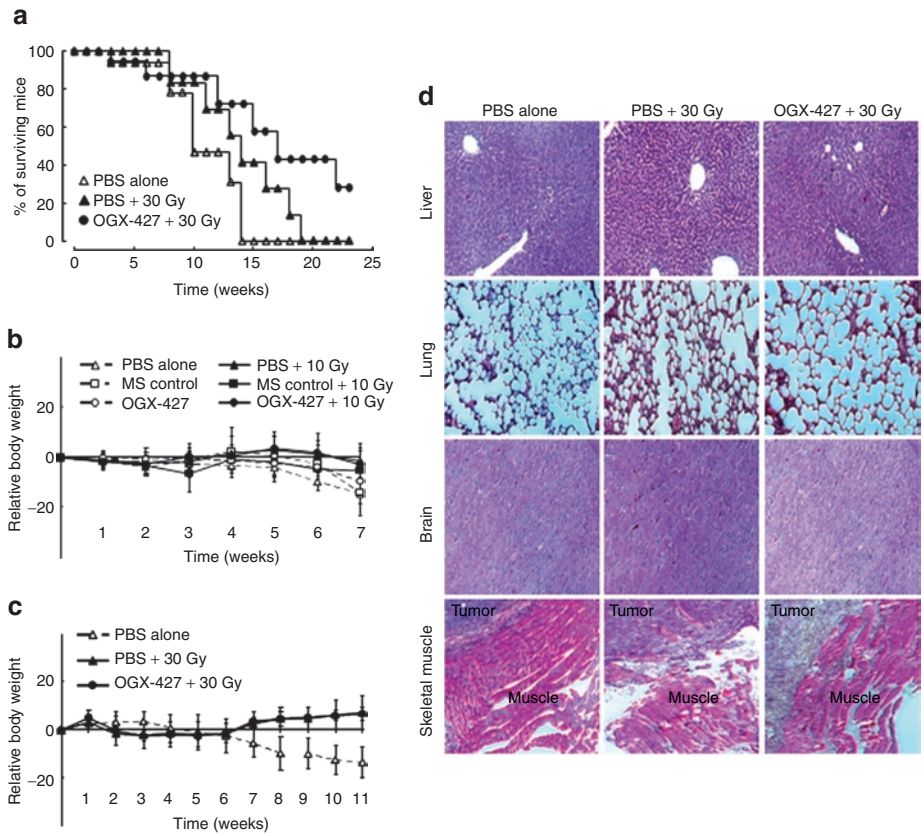

Figure 3 Combined therapy increases the survival of mice without significant toxicity. (**a**) The Kaplan–Meyer survival curves represent the percentage of mice alive at the indicated time points for each group of the experiment II. (**b**) Body weight monitoring of mice after treatment with PBS, MS-control, or OGX-427 oligonucleotides associated or not with 10 Gy irradiation (experiment I). (**c**) Body weight monitoring after treatment with PBS associated or not with 30 Gy irradiation, and OGX-427 + 30 Gy (experiment II). Body weight was measured once weekly and results were expressed as mean ± SD relative to that measured at the beginning of treatment. (**d**) Tissue morphology of liver, lung, brain, and muscle surrounding tumors assessed on paraffin-embedded tissue sections after hematoxylin, phloxine, and saffron staining (week 6, experiment II). Magnification ×100. PBS, phosphate-buffered saline.

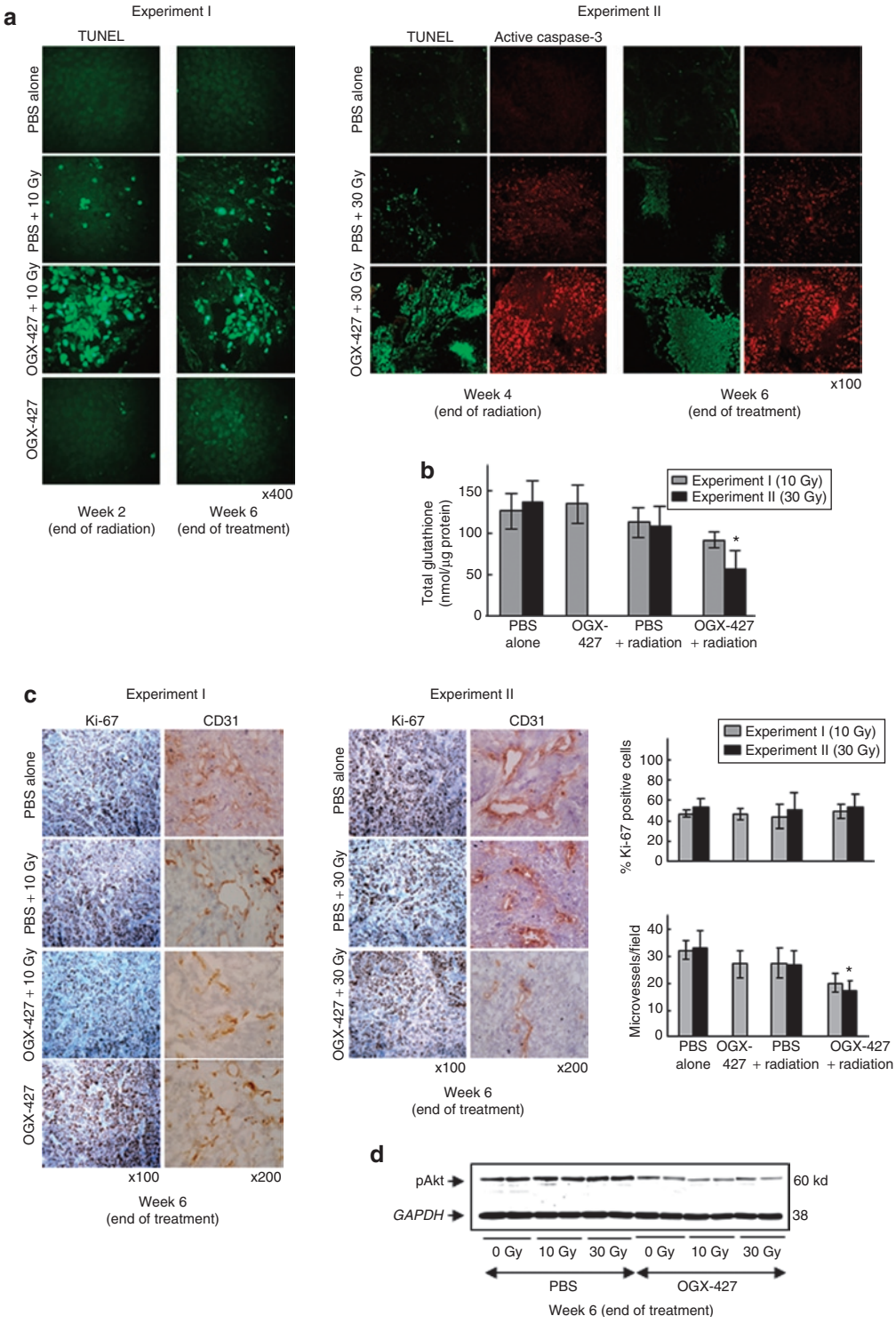

Figure 4 Hsp27 knockdown by OGX-427 combined with irradiation induces apoptosis, decreases intratumoral glutathione levels and angiogenesis, without altering cell proliferation. (**a**) Detection of apoptosis using TUNEL and active-caspase-3 staining on paraffin-embedded tumor sections (×400 or ×100 magnification). (**b**) Total glutathione levels measured by HPLC on tumors collected at the end of treatment from both experiments. Each value represents the mean ± SD of triplicate samples for each collected tumor. *$P < 0.05$ versus 30 Gy irradiated tumors. (**c**) Detection of tumor cell proliferation and angiogenesis using respectively Ki-67 and CD31 immunostaining on tumors taken at the end of treatment from both experiments (×100 or ×200 magnification). The proliferative index was calculated as the percentage of Ki-67 positive cells counted in 20 random fields at ×400 magnification for each tumor. The MVD (microvessel density) was quantified by counting the number of microvessels in 10 random fields at ×200 magnification for each tumor. *$P < 0.05$ versus 30 Gy irradiated tumors. (**d**) Immunoblot analysis of the phosphorylated active form of Akt (pAkt) in SQ20B xenograft tumors at the end of treatment (two different tumors per group). Protein (10 µg) was loaded on the gels. GAPDH, glyceraldehyde-3-phosphate-dehydrogenase; HPLC, high-performance liquid chromatography; Hsp, heat shock protein; PBS, phosphate-buffered saline; TUNEL, terminal nucleotidyl transferase–mediated nick end labeling.

vascularization using, respectively, Ki-67 and CD31 immunostaining of tumors taken at week 6. Despite a tendency to a lower proliferation index was deduced from microscopic observation, the quantitative analysis with the Histolab-Microvision Image Analysis software (Microvision Instruments, Evry, France) showed no significant variation of the proliferative index (% of Ki-67 positive cells) between all treatment groups from both experiments (**Figure 4c**).

In contrast, immunohistochemical staining for CD31 revealed a significant decrease in vessel count in tumors from the combination therapy group of OGX-427 plus radiation, most evident following the 30 Gy associated treatment (38% compared to only irradiated mice group, $^*P < 0.05$). Mice that received radiation or OGX-427 alone exhibited a slight decrease in tumor angiogenesis (**Figure 4c**). Because Akt can promote angiogenesis by regulating the expression of vascular endothelial growth factor and because Hsp27 knockdown inhibits Akt activation in cultured cells, we investigated whether the decrease of angiogenesis observed in xenograft tumors treated with OGX-427 plus radiation could be explained by a decrease in Akt activity. Western blot analysis revealed a decrease of the phosphorylated active form of Akt (pAkt) in tumors treated with OGX-427 associated or not with irradiation compared to those receiving no OGX-427 treatment (**Figure 4d**).

Thus, OGX-427 downregulation of Hsp27 in combination with radiation significantly enhances apoptosis associated with a decrease of both antioxidant defenses and tumor vascularization.

DISCUSSION

Modulation of the expression of antiapoptotic proteins by specific antisense oligonucleotides (ASOs) in association to current cancer therapies seems a promising therapeutic approach. Hsp27 overexpression in tumors, coupled with its role in resistance to chemotherapy and radiation therapy–induced apoptosis, makes it an interesting target for anticancer therapy.

The highly dynamic formation of oligomers of up to 1,000 kd seems to play a central role in regulating the chaperone[19] and tumorigenic[20] activities of Hsp27. Through its chaperone activity, Hsp27 regulates apoptosis by its ability to interact with key components of the apoptotic signaling pathways.[21] It inhibits the cytochrome *c* release,[22] prevents the formation of the apoptosome, and the subsequent activation of procaspase-9 and procaspase-3 (refs. 23,24). In addition, Hsp27 maintains the actin network integrity and hence prevents the translocation of pro-apoptotic factors such as activated Bid (tBid) onto the mitochondrial membrane.[25] Hsp27 can also block Daxx-mediated apoptosis by preventing its translocation to the plasma membrane and thus inhibiting its interaction with Fas and Ask-1 (ref. 26). Havasi *et al.* have recently shown that Hsp27 is also able to antagonize Bax-mediated mitochondrial injury and apoptosis by promoting Akt activation via a phosphatidylinositol-3-kinase-dependant mechanism.[18] Thus, the knockdown of Hsp27 expression would affect multiple pathways implicated in cancer cell survival and the resistance to chemotherapy and radiotherapy treatment. Conversely, increasing the expression of Hsp27 protein might be useful in the therapeutic strategy of certain forms of neurodegenerative diseases, as it has been identified as a potent protective factor in neuronal cells.[27] Furthermore, mutations of Hsp27 gene have been associated to mild clinical form of Charcot-Marie-Tooth disease and to hereditary motor neuropathy type II.[28]

In this study, we evaluated, *in vivo*, the potential radiosensitizing effect of the 2′-methoxyethyl modified phosphorothioate ASO OGX-427 on SQ20B tumors. In SQ20B cultured cells, the knockdown of Hsp27 by OGX-427 combined with irradiation led to increased levels of apoptotic and clonogenic cell death, and decreased activation of the Akt survival pathway. *In vivo*, compared with untreated control, the administration of OGX-427 combined with tumor irradiation resulted in a drastic regression of SQ20B tumors and enhanced survival of SQ20B-bearing mice without significant tissue damage or toxicity. The significant decrease of tumor growth is due in large part to the high level of induction of radiation-induced apoptosis after OGX-427 treatment, closely associated with a decrease in the antioxidant defenses. We have demonstrated for the first time that, *in vivo*, knockdown of Hsp27 in combination with irradiation leads to a significant decrease in intratumoral glutathione levels. Our results confirm previous observations[10] demonstrating the ability of Hsp27 to enhance the antioxidant defenses of tumor cells by maintaining cellular glutathione content. They also clearly show that the induction of apoptosis is a critical determinant of tumor radiosensitivity.

Rocchi *et al.* have shown that treatment with Hsp27 antisense delays the tumor progression of androgen-independent[29] and androgen-sensitive[30] prostate xenografts. In prostate cancer, the anticancer effect of OGX-427 treatment on tumor growth occurs, in part, via inhibition of cooperative interaction between ligand-activated androgen receptor and Hsp27 (ref. 31). Contrary to these results, treatment by OGX-427 alone or combined with radiation exhibited no effect on SQ20B tumor proliferation, as no difference in the proliferative index (% Ki-67 positive cells) was observed between all treatment groups.

However, we described a significant decrease of angiogenesis in tumors treated with OGX-427 associated with irradiation. Hsp27 has been described as a potential positive regulator of vessel growth.[32] On the other hand, Pore *et al.* have recently described a decrease of angiogenesis in SQ20B xenografts treated with irradiation plus nelfinavir, an inhibitor of the phosphatidylinositol-3-kinase/Akt pathway.[33] Moreover, the phosphatidylinositol-3-kinase/Akt pathway has been implicated in the regulation of vascular endothelial growth factor expression and consequently of tumor angiogenesis. Because Hsp27 regulates Akt activation in stressed cells[34] and because we have confirmed the absence of Akt activation in Hsp27 under-expressing tumors, we can postulate that the decrease of tumor vascularization observed in tumors treated with OGX-427 may result from a decrease in vascular endothelial growth factor promoter activation.

Our results are in good agreement with those found in bladder cancer reported by Kamada *et al.*, showing the efficiency of the Hsp27 inhibiting strategy with OGX-427 treatment in combination with chemotherapy.[35] This study represents the first *in vivo* demonstration of the efficacy of Hsp27 antisense in combination with radiation for cancer therapy.

Inhibition of other antiapoptotic proteins such as survivin[36] and X-linked inhibitor of apoptosis protein[37] by ASOs has also proved successful in reducing tumor growth and increasing the

rates of apoptosis of different xenograft tumors. The ASO targeting Bcl-2 antiapoptotic protein has also been successfully used in this fashion against cancers in both human xenograft tumor models and cancer patients.[38,39] Despite the somewhat disappointing results of recent antisense oncology trials, ongoing progress in ASO technology with improvements in tumor targeted delivery have raised new hopes of enhancing clinical efficacy.[40] The 2′-methoxyethyl modified second-generation phosphorothioate ASOs have already proved their efficiency in cancer therapy. In this way, OGX-011, an ASO targeting clusterin, has been evaluated in several phase I and II clinical trials in combination with docetaxel for the treatment of prostate, lung, and breast cancers.[41] A phase I clinical study evaluating OGX-427 combined with docetaxel in patients with advanced cancers has also just begun.

In light of our results, Hsp27 knockdown using OGX-427 in combination with radiotherapy seems to be another viable therapeutic approach for clinical application. These results provide a basis for the clinical utility of the Hsp27 antisense approach associated to γ-radiation in the treatment of patients with cancers resistant to radiotherapy such as HNSCC.

MATERIALS AND METHODS

In vitro *treatments.* The HNSCC SQ20B cells were established from a patient with recurrent squamous cell carcinoma of the larynx after radiation therapy[42] and cultured as previously reported.[43]

Cells were irradiated at room temperature on a Clinac C/D-600 (Varian Medical Systems, Palo Alto, CA) at a general dose of 10 Gy delivered at a dose rate of 2 Gy/min with photon energy of 6 MV.

The second-generation 2′-*O*-(2-methoxyethyl) ASO against Hsp27 (OGX-427) was kindly supplied by Oncogenex Technologies (Vancouver, British Columbia, Canada). The sequence of OGX-427 corresponds to the human Hsp27 translation initiation site (5′-GGGACGCGGCG CTCGGTCAT-3′). An MS (5′-CAGCGCTGACAACAGTTTCAT-3′) was used as control. Cells were treated for 2 days with 200 nmol/l OGX-427 or MS-control after a preincubation for 20 minutes with 3.5 μg/ml oligofectamine (Invitrogen, Carlsbad, CA) in serum-free OPTI-MEM (Invitrogen).

Clonogenic assay. Cell survival curves were generated by means of a standard colony formation assay, as previously described.[44] The survival fraction at 2 Gy was determined as an index of radiosensitivity.

Cell apoptosis. Total cellular caspase activity was quantified by flow cytometry after labeling with the CaspACE FITC-VAD-FMK in Situ Marker (Promega, Charbonnières, France). Apoptotic cellular morphologic characteristics were visualized by means of 4′-6-diamidino-2-phenylindole-dihydrochloride staining as previously described.[13]

In vivo *treatments.* A suspension of 3×10^6 SQ20B cells in 200 μl of PBS was subcutaneously inoculated in the right flank region of 5-week-old female athymic nude mice (Charles River Laboratories, L'Arbresle, France) via a 23-gauge needle under ketamine/xylazine anesthesia. All animal procedures were performed according to local guidelines on animal care. When the tumor reached 300–400 mm^3 in volume, mice were randomly selected for treatment. Two successive experiments were conducted in which the administered treatment differed by the total dose of irradiation. Ten mg/kg of OGX-427 or MS-control were injected intraperitoneally once daily for 5 successive days (week 1), then one injection every 2 days during the 5 following weeks. Local tumor irradiation was performed under ketamine/xylazine anesthesia from the beginning of week 2 at a dose rate of 2 Gy/min. A 2 Gy dose was delivered daily for 5 days (10 Gy total) in the first study (experiment I), with the protocol repeated during weeks 3 and 4 (30 Gy total) for the second (experiment II). The 5 × 2 Gy fractionated radiation dose was used to mimic the protocol classically applied to a patient for a week of treatment. Experiment I consisted of 6 groups of 10 mice: PBS-alone, MS-control, OGX-427, PBS + 10 Gy, MS + 10 Gy, and OGX-427 + 10 Gy. Experiment II included three groups of 16 mice: PBS-alone, PBS + 30 Gy, and OGX-427 + 30 Gy. Clinical observations were carried out daily alongside weekly measurements of body weight and tumor volume, which was calculated according to the formula: $0.5236\ (L \times W^2)$, where L and W are, respectively, the length and width diameters. For each mice group, histological and biochemical analyses were performed on tumors taken after being killed at the end of irradiation (week 2 for experiment I, week 4 for experiment II) and at the end of treatment (week 6 for both experiments). Mice were killed at desired time points. Several aliquots of tumors were immediately frozen in liquid nitrogen or fixed in 4% formalin for 24 hours and embedded in paraffin. Mice were killed when tumors reached a considerable size.

Biochemical analyses. Immunoblot analysis of protein extracts was performed as described previously.[13] The primary monoclonal antibodies were anti-Hsp27, anti-Hsp70, and anti-Hsp90 (Santa-Cruz Biotechnologies, Santa-Cruz, CA), anti-pAKt (pS473) (Epitomics, Burlingame, CA), and antiglyceraldehyde-3-phosphate-dehydrogenase (Biodesign-International, Saco, ME). The horseradish-peroxidase (HRP)-conjugated secondary antibodies were from Santa-Cruz. Densitometric analysis was performed using 1DScan-EX3.1 software (Scanalytics, Fairfax, VA).

Total glutathione was quantified from tumor extracts prepared as previously described and separated by high-performance liquid chromatography with fluorimetric detection.[43]

Histological analyses. The tissue morphology of liver, lung, brain, and muscle surrounding the tumors was assessed on formalin-fixed, paraffin-embedded tissue sections after hematoxylin, phloxine, and saffron staining.

Immunohistochemical analyses.

Terminal nucleotidyl transferase–mediated nick end labeling: Terminal nucleotidyl transferase–mediated nick end labeling staining was carried out on formalin-fixed, paraffin-embedded tissue sections (5 μm) with the DeadEnd Fluorometric TUNEL System (Promega) according to the manufacturer's instructions. Slides were examined using an Olympus-BX41 microscope (Olympus America, Center Valley, PA) and images taken at ×100 or ×400 magnification using a Nikon digital camera (Nikon, Melville, NY).

Cell proliferation and expression of cleaved-caspase-3: Tumor sections (5 μm) were hydrated through xylene and graded ethanol and equilibrated in PBS before undergoing antigen retrieval. Endogene peroxidase activity was quenched and tissue sections were incubated with a mouse-monoclonal anti-Ki-67 (clone-MIB1; DAKO, Glostrup, Denmark) for cell proliferation study, or a rabbit-monoclonal antiactive-caspase-3 (Epitomics) at a dilution of 1/50 for 1 hour at room temperature. The appropriate secondary antibodies were HRP-conjugated for Ki-67 and rhodamine-conjugated for cleaved-caspase-3. HRP detection was achieved with 3,3′-diaminobenzidine substrate (Sigma, St Quentin Fallavier, France) and counterstained with hematoxylin (Sigma). The proliferative index was calculated as the percentage of Ki-67 positive cells counted in 20 random fields at ×400 magnification for each tumor (one slide/mouse, 2 or 3 slides/group) on an Eclipse-E400 microscope (Nikon) equipped with a three-chip-charge coupled device color video camera (DXC-390P; Sony, Tokyo, Japan) and Histolab-Microvision Image Analysis software.

Tumor angiogenesis: Tumor angiogenesis was analyzed on 7-μm freshly cut sections of frozen tumors. After fixation in cold acetone, endogene peroxidase activity was quenched and tissue sections were incubated with a rat-anti-mouse CD31 (clone MEC-13.3; BD Pharmingen, San Diego, CA) at a dilution of 1/50. After incubation for 30 minutes each with

biotin goat-anti-rat IgG, and HRP-conjugated Ultra-Streptavidin (BD Pharmingen), HRP detection was achieved as described above and counterstained with hematoxylin. The microvessel density was quantified by counting the number of microvessels in 10 random fields at ×200 magnification for each tumor (one slide/mouse, 2 or 3 slides/group).

Statistical analysis. All results are expressed as the mean ± SD. Statistical significance was tested using Student's *t*-test (Excel-Microsoft, Courtaboeuf, France); degree of statistical significance: $P < 0.05$ was considered significant. $^{*}P < 0.05$; $^{**}P < 0.005$; $^{***}P < 0.001$.

ACKNOWLEDGMENTS

This work was supported by the Ligue contre le Cancer (Comités de de l'Ain et de Savoie), and ETOILE (Contrat de Plan Etat-Région). Elie Hadchity was supported by a grant from the Ligue contre le Cancer (Comité de la Saône et Loire). We thank the radiophysicists from the Radiotherapy Department, Irénée Sentenac, Patrice Jalade, Anne-Lise Vercheyre, and Mathieu Bernadi for their help with animal irradiations. We thank Jean-Yves Scoazec (Pathological Anatomy and Cytology Department, Edouard Herriot Hospital) for allowing us access to the Histolab-Microvision Image Analysis software. We thank Colette Berthet for her help in the quantification of glutathione (Laboratoire de Biochimie, Centre de Biologie Est, Lyon, France).

REFERENCES

1. Bourhis, J, Etessami, A and Lusinchi, A (2005). New trends in radiotherapy for head-and-neck-cancer. *Ann Oncol* **16**(Suppl 2): ii255–ii257.
2. Miyake, H, Muramaki, M, Kurahashi, T, Yamanaka, K, Hara, I and Fujisawa, M (2006). Enhanced expression of heat shock protein 27 following neoadjuvant hormonal therapy is associated with poor clinical outcome in patients undergoing radical prostatectomy for prostate cancer. *Anticancer Res* **26**:1583–1587.
3. Thanner, F, Sütterlin, MW, Kapp, M, Rieger, L, Morr, AK, Kristen, P *et al.* (2005). Heat shock protein 27 is associated with decreased survival in node-negative breast cancer patients. *Anticancer Res* **25**:1649–1653.
4. Kapranos, N, Kominea, A, Konstantinopoulos, PA, Savva, S, Artelaris, S, Vandoros, G *et al.* (2002). Expression of the 27-kDa heat shock protein (HSP27) in gastric carcinomas and adjacent normal, metaplastic, and dysplastic gastric mucosa, and its prognostic significance. *J Cancer Res Clin Oncol* **128**:426–432.
5. Lebret, T, Watson, RW, Molinié, V, O'Neill, A, Gabriel, C, Fitzpatrick, JM *et al.* (2003). Heat shock proteins HSP27, HSP60, HSP70, and HSP90: expression in bladder carcinoma. *Cancer* **98**:970–977.
6. Lo, WY, Tsai, MH, Tsai, Y, Hua, CH, Tsai, FJ, Huang, SY *et al.* (2007). Identification of over-expressed proteins in oral squamous cell carcinoma (OSCC) patients by clinical proteomic analysis. *Clin Chim Acta* **376**:101–107.
7. Storm, FK, Mahvi, DM and Gilchrist, KW (1996). Heat shock protein 27 overexpression in breast cancer lymph node metastasis. *Ann Surg Oncol* **3**:570–573.
8. Romani, AA, Crafa, P, Desenzani, S, Graiani, G, Lagrasta, C, Sianesi, M *et al.* (2007). The expression of Hsp27 is associated with poor clinical outcome in intrahepatic cholangiocarcinoma. *BMC Cancer* **7**:232.
9. Vargas-Roig, LM, Gago, FE, Tello, O, Aznar, JC and Ciocca, DR (1998). Heat shock protein expression and drug resistance in breast cancer patients treated with induction chemotherapy. *Int J Cancer* **79**:468–475.
10. Kassem, HSh, Sangar, V, Cowan, R, Clarke, N and Margison, GP (2002). A potential role of heat shock proteins and nicotinamide N-methyl transferase in predicting response to radiation in bladder cancer. *Int J Cancer* **101**:454–460.
11. Teimourian, S, Jalal, R, Sohrabpour, M and Goliaei, B (2006). Down-regulation of Hsp27 radiosensitizes human prostate cancer cells. *Int J Urol* **13**:1221–1225.
12. Préville, X, Salvemini, F, Giraud, S, Chaufour, S, Paul, C, Stepien, G *et al.* (1999). Mammalian small stress proteins protect against oxidative stress through their ability to increase glucose-6-phosphate-dehydrogenase activity and by maintaining optimal cellular detoxifying machinery. *Exp Cell Res* **247**:61–78.
13. Alphonse, G, Aloy, MT, Broquet, P, Gerard, JP, Louisot, P, Rousson, R *et al.* (2002). Ceramide induces activation of the mitochondrial/caspases pathway in Jurkat and SCC61 cells sensitive to γ-radiation but activation of this sequence is defective in radioresistant SQ20B cells. *Int J Radiat Biol* **78**:821–835.
14. Aloy, MT, Hadchity, E, Bionda, C, Diaz-Latoud, C, Claude, L, Rousson, R *et al.* (2008). Protective role of Hsp27 protein against γ radiation-induced apoptosis and radiosensitization effects of Hsp27 gene silencing in different human tumor cells. *Int J Radiat Oncol Biol Phys* **70**:543–553.
15. Rane, MJ, Pan, Y, Singh, S, Powell, DW, Wu, R, Cummins, T *et al.* (2003). Heat shock protein 27 controls apoptosis by regulating Akt activation. *J Biol Chem* **278**: 27828–27835.
16. Wu, R, Kausar, H, Johnson, P, Montoya-Durango, DE, Merchant, M and Rane, MJ (2007). Hsp27 regulates Akt activation and polymorphonuclear leukocyte apoptosis by scaffolding MK2 to Akt signal complex. *J Biol Chem* **282**:21598–21608.
17. Osaki, M, Oshimura, M and Ito, H (2004). PI3K-Akt pathway: its functions and alterations in human cancer. *Apoptosis* **9**:667–676.
18. Havasi, A, Li, Z, Wang, Z, Martin, JL, Botla, V, Ruchalski, K *et al.* (2008). Hsp27 inhibits Bax activation and apoptosis via a PI3 kinase-dependent mechanism. *J Biol Chem* **283**:12305–12313.
19. Rogalla, T, Ehrnsperger, M, Preville, X, Kotlyarov, A, Lutsch, G, Ducasse, C *et al.* (1999). Regulation of Hsp27 oligomerization, chaperone function, and protective activity against oxidative stress/tumor necrosis factor α by phosphorylation. *J Biol Chem* **274**:18947–18956.
20. Bruey, JM, Paul, C, Fromentin, A, Hilpert, S, Arrigo, AP, Solary, E *et al.* (2000). Differential regulation of HSP27 oligomerization in tumor cells grown *in vitro* and *in vivo*. *Oncogene* **19**:4855–4863.
21. Garrido, C, Gurbuxani, S, Ravagnan, L and Kroemer, G (2001). Heat shock proteins: endogenous modulators of apoptotic cell death. *Biochem Biophys Res Commun* **286**:433–442.
22. Bruey, JM, Ducasse, C, Bonniaud, P, Ravagnan, L, Susin, SA, Diaz-Latoud, C *et al.* (2000). HSP27 negatively regulates cell death by interacting with cytochrome c. *Nat Cell Biol* **2**:645–652.
23. Garrido, C, Bruey, JM, Fromentin, A, Hammann, A, Arrigo, AP and Solary, E (1999). HSP27 inhibits cytochrome c-dependent activation of procaspase-9. *FASEB J* **13**:2061–2670.
24. Pandey, P, Farber, R, Nakazawa, A, Kumar, S, Bharti, A, Nalin, C *et al.* (2000). Hsp27 functions as a negative regulator of cytochrome c-dependent activation of procaspase-3. *Oncogene* **19**:1975–1981.
25. Paul, C, Manero, F, Gonin, S, Kretz-Remy, C, Virot, S and Arrigo, AP (2002). Hsp27 as a negative regulator of cytochrome C release. *Mol Cell Biol* **22**:816–834.
26. Charrette, SJ, Lavoie, JN, Lambert, H and Landry, J (2000). Inhibition of Daxx-mediated apoptosis by heat shock protein 27. *Mol Cell Biol* **20**:7602–7612.
27. Latchman, DS (2005). HSP27 and cell survival in neurones. *Int J Hyperthermia* **21**:393–402.
28. Houlden, H, Laura, M, Wavrant-De Vrièze, F, Blake, J, Wood, N and Reilly, MM (2008). Mutations in the HSP27 (HSPB1) gene cause dominant, recessive, and sporadic distal HMN/CMT type 2. *Neurology* **71**:1660–1668.
29. Rocchi, P, So, A, Kojima, S, Signaevsky, M, Beraldi, E, Fazli, L *et al.* (2004). Heat shock protein 27 increases after androgen ablation and plays a cytoprotective role in hormone-refractory prostate cancer. *Cancer Res* **64**:6595–6602.
30. Rocchi, P, Beraldi, E, Ettinger, S, Fazli, L, Vessella, RL, Nelson, C *et al.* (2005). Increased Hsp27 after androgen ablation facilitates androgen-independent progression in prostate cancer via signal transducers and activators of transcription 3-mediated suppression of apoptosis. *Cancer Res* **65**:11083–11093.
31. Zoubeidi, A, Zardan, A, Beraldi, E, Fazli, L, Sowery, R, Rennie, P *et al.* (2007). Cooperative interactions between androgen receptor (AR) and heat-shock protein 27 facilitate AR transcriptional activity. *Cancer Res* **67**:10455–10465.
32. Piotrowicz, RS, Martin, JL, Dillman, WH and Levin, EG (1997). The 27-kDa heat shock protein facilitates basic fibroblast growth factor release from endothelial cells. *J Biol Chem* **272**:7042–7047.
33. Pore, N, Gupta, AK, Cerniglia, GJ, Jiang, Z, Bernhard, EJ, Evans, SM *et al.* (2006). Nelfinavir down-regulates hypoxia-inducible factor 1α and VEGF expression and increases tumor oxygenation: implications for radiotherapy. *Cancer Res* **66**: 9252–9259.
34. Zhang, Y and Shen, X (2007). Heat shock protein 27 protects L929 cells from cisplatin-induced apoptosis by enhancing Akt activation and abating suppression of thioredoxin reductase activity. *Clin Cancer Res* **13**:2855–2864.
35. Kamada, M, So, A, Muramaki, M, Rocchi, P, Beraldi, E and Gleave, M (2007). Hsp27 knockdown using nucleotide-based therapies inhibit tumor growth and enhance chemotherapy in human bladder cancer cells. *Mol Cancer Ther* **6**:299–308.
36. Rödel, F, Frey, B, Leitmann, W, Capalbo, G, Weiss, C and Rödel, C (2008). Survivin antisense-oligonucleotides effectively radiosensitize colorectal cancer cells in both tissue culture and murine xenograft models. *Int J Radiat Oncol Biol Phys* **71**:247–255.
37. LaCasse, EC, Cherton-Horvat, GG, Hewitt, KE, Jerome, LJ, Morris, SJ, Kandimalla, ER *et al.* (2006). Preclinical characterization of AEG35156/GEM 640, a second-generation antisense oligonucleotide targeting X-linked inhibitor of apoptosis. *Clin Cancer Res* **12**:5231–5241.
38. Yip, KW, Mocanu, JD, Au, PY, Sleep, GT, Huang, D, Busson, P *et al.* (2005). Combination bcl-2 antisense and radiation therapy for nasopharyngeal cancer. *Clin Cancer Res* **11**:8131–8144.
39. Piro, LD (2004). Apoptosis, Bcl-2 antisense, and cancer therapy. *Oncology* **18**:5–10.
40. Gleave, ME and Monia, BP (2005). Antisense therapy for cancer. *Nat Rev Cancer* **5**:468–479.
41. Chi, KN, Siu, LL, Hirte, H, Hotte, SJ, Knox, J, Kollmansberger, C *et al.* (2008). A phase I study of OGX-011, a 2′-methoxyethyl phosphorothioate antisense to clusterin, in combination with docetaxel in patients with advanced cancer. *Clin Cancer Res* **14**:833–839.
42. Weichselbaum, RR, Dahlberg, W, Beckett, M, Karrison, T, Miller, D, Clark, J *et al.* (1986). Radiation-resistant and repair-proficient human tumor cells may be associated with radiotherapy failure in head-and-neck-cancer patients. *Proc Natl Acad Sci USA* **83**:2684–2688.
43. Rodriguez-Lafrasse, C, Alphonse, G, Broquet, P, Aloy, MT, Louisot, P and Rousson, R (2001). Temporal relationships between ceramide production, caspase activation and mitochondrial dysfunction in cell lines with varying sensitivity to anti-Fas-induced-apoptosis. *Biochem J* **357**:407–416.
44. Alphonse, G, Bionda, C, Aloy, MT, Ardail, D, Rousson, R and Rodriguez-Lafrasse, C (2004). Overcoming resistance to γ-rays in squamous carcinoma cells by poly-drug elevation of ceramide levels. *Oncogene* **23**:2703–2715.